Supporting Information

Riley A. Suhar[a], Vanessa M. Doulames[a,b], Yueming Liu[a], Meghan E. Hefferon[a,b], Oscar Figueroa III[c], Hana Buabbas[a,d], Sarah C. Heilshorn[a*]

[a] Department of Materials Science and Engineering, Stanford University, Stanford, California 94305, USA

[b] Department of Neurosurgery, Stanford University School of Medicine, Stanford, California 94305, United States

[c] Ellicott City, Maryland 21043, USA, ozzief@alum.mit.edu

[d] Department of Biology, Stanford University, Stanford, California, 94305, United States

[*] Corresponding author.
E-mail: heilshorn@stanford.edu (S.C.H.)
Address: 476 Lomita Mall, McCullough Room 246, Stanford University.
Stanford, CA, 94305-4045, USA
Fax Number: 650-723-3044

Summary:

A

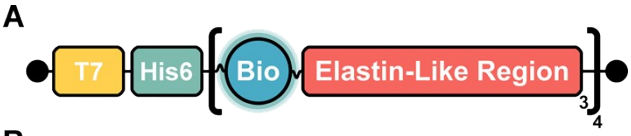

B

Elastin-Like Protein Amino Acid Sequence	
Component	**Sequence**
T7-tag	*MASMTGGQQMG*
Polyhistidine-tag	*HHHHHH*
Bio-Active Region	*TVYAVTGRGDSPASS*
Elastin-Like Region	*$(VPGIV)_2(VPGKG)(VPGIG)_2$*

Figure S1. Elastin-like protein amino acid sequence information: *(A) A schematic representation of the elastin-like protein (ELP) used in the present manuscript. Our ELP contains three key-components: (1) a tag region with a T7-tag and Polyhistidine-tag, (2) a bio-active domain and (3) an elastin-like region. (B) The amino acid sequence for these components are included for reference.*

NMR Quantification:

Hydrazine functionalization: dissolve ~10 mg of the Boc-protected ELP-Hydrazine intermediate in ~750 µL deuterated DMSO and analyze by 1H NMR (500 Hz, DMSO-d6): Tetramethyl silane (TMS; 0). Efficiency of modification is determined by comparing the integrated signal of the Boc protons (27H; δ 1.5-1.35) to the aromatic protons of tyrosine residues on ELP (8H each; centered at δ 7.00 and 6.62).

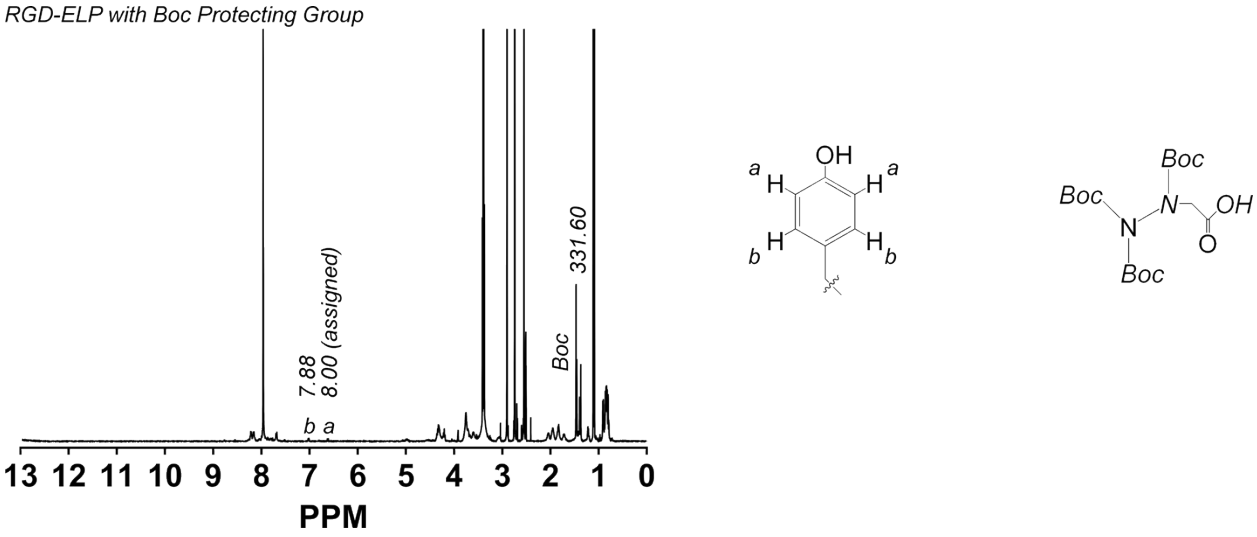

Figure S2. NMR quantification of modification efficiency for ELP-Hydrazine: *NMR of Boc-protected ELP indicates approximatly 12.28 hydrazine moities are present per ELP chain.*

A

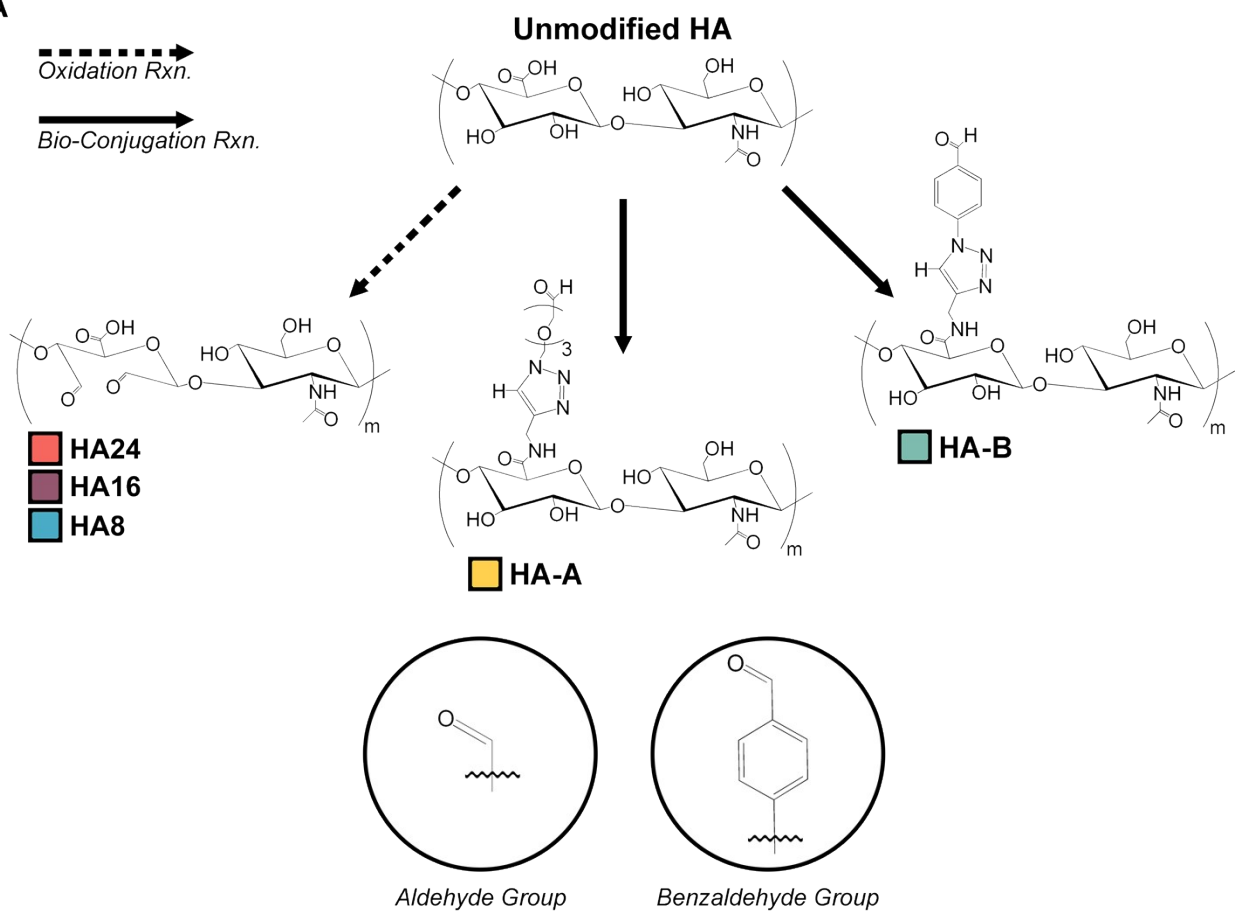

B

Hydrogel Summary			
Hydrogel	**Starting M_w**	**Modification Scheme**	**Bond Kinetics**
HA24	*1.5 MDa*	*Oxidation (24 hr)*	*Fast*
HA16	*1.5 MDa*	*Oxidation (16 hr)*	*Fast*
HA8	*1.5 MDa*	*Oxidation (8 hr)*	*Fast*
HA-A	*100 kDa*	*Bio-Conjugation*	*Fast*
HA-B	*100 kDa*	*Bio-Conjugation*	*Slow*

Figure S3. Summary of conjugation and oxidation reactions for hyaluronan: (A) *A schematic representation of our different hyaluronan (HA) components. Three variants were produced by oxidizing 1.5 MDa HA for 24 hr (HA24), 16 hr (HA16), and 8 hr (HA8). The other two HA variants were produced* via *2-part bio-conjugation reaction wherein 100 kDa HA was first reacted to have 12% of the HA repeat groups modified with an alkyne group (HA-Alkyne). A secondary reaction then conjugated a small molecule with either a pendant aldehyde (HA-A) or benzaldehyde group (HA-B) to the alkyne through a copper-click reaction. (B) A summary of our HA groups and relevant properties have been summarized.*

2,4,6-Trinitrobenzene Sulfonic Acid (TNBS) Assay:

The degree of HA oxidation for our oxidized HA variants (HA24, HA16, and HA8) was measured using a modified TNBS assay, as previously described [1]. HA samples were dissolved in ultra pure DI water at 0.6% (w/v) overnight. The following morning, 25 µL of HA was mixed with 25 µL tert-butyl carbazate (t-BC; 30 mM; 1% aqueous trichloroacetic acid; Sigma, B91005) and left to react for 24 hr at room temperature in the dark. The following day, 5 µL of sample was diluted with 995 µL sodium bicarbonate buffer (0.1M, pH 8.5). 500 µL of diluted sample was then mixed with 250 µL aqueous TNBS (0.1%, diluted with 0.1M sodium bicarbonate; Thermo, 28997) and left to react with the excess t-BC for 2 hr at 37 °C. The reaction was stopped by the careful addition of 125 µL of 1 M hydrochloric acid, and 100 µL of the mixture was finally transferred into a 96-well assay plate. The absorbance at 340 nm was measured using a SpectraMax M2 microplate reader. A standard calibration curve made from the aqueous t-BC solutions (1 – 20 mM; diluted with 0.1M sodium bicarbonate) was used to determine the amount of unreacted t-BC and to convert the result into di-aldehyde content. All measurements were repeated in triplicate.

A

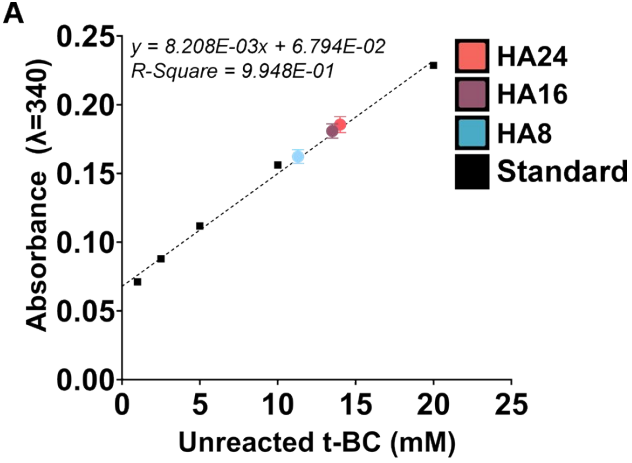

B

Oxidation Summary		
Hydrogel	**Absorbance**	**Oxidation (Avg.)**
HA24	*0.185 ± 0.006*	*10.4%*
HA16	*0.181 ± 0.005*	*14.1%*
HA8	*0.162 ± 0.005*	*29.2%*

Figure S4. TNBS assay for measuring degree of oxidation: *The dialdehyde content of our oxidized variants (HA24, HA16, and HA8) were determined through a modified, two-part, TNBS assay. First, the aldehyde groups were reacted with a known quantity of tert-butyl carbazate (t-BC) to form a stable carbazone. The remaining unreacted, t-BC content was determined by subsequent reaction with TNBS, which forms a chromogenic derivative that can be detected at λ = 340 nm. (A) Our measurements (in triplicate) are plotted against a standard curve. (B) The results are further summarized in a table below for ease of comparison.*

NMR Quantification:

Aldehyde functionalization: dissolve ~10 mg of HA-Aldehyde (HA-A) in ~750 µL of D_2O and analyze by 1H NMR (500 Hz, D_2O): TMS (0); Acetyl group (3H, δ ~1.8); water (δ ~4.7); triazole (1H; δ ~7.85). To quantify the degree of modification, compare the integrated peak of the triazole group to the acetyl group.

Benzaldehyde functionalization: dissolve ~10 mg of HA-Benzaldehyde (HA-B) in ~750 µL of D_2O and analyze by 1H NMR (500 Hz, D_2O): TMS (0); Acetyl group (3H, δ ~1.8); water (δ ~4.7); triazole (1H) and aldehyde group (1H δ ~9.8 ~ 9.9). To quantify the degree of modification, compare the integrated peak of the aldehyde proton to the acetyl group.

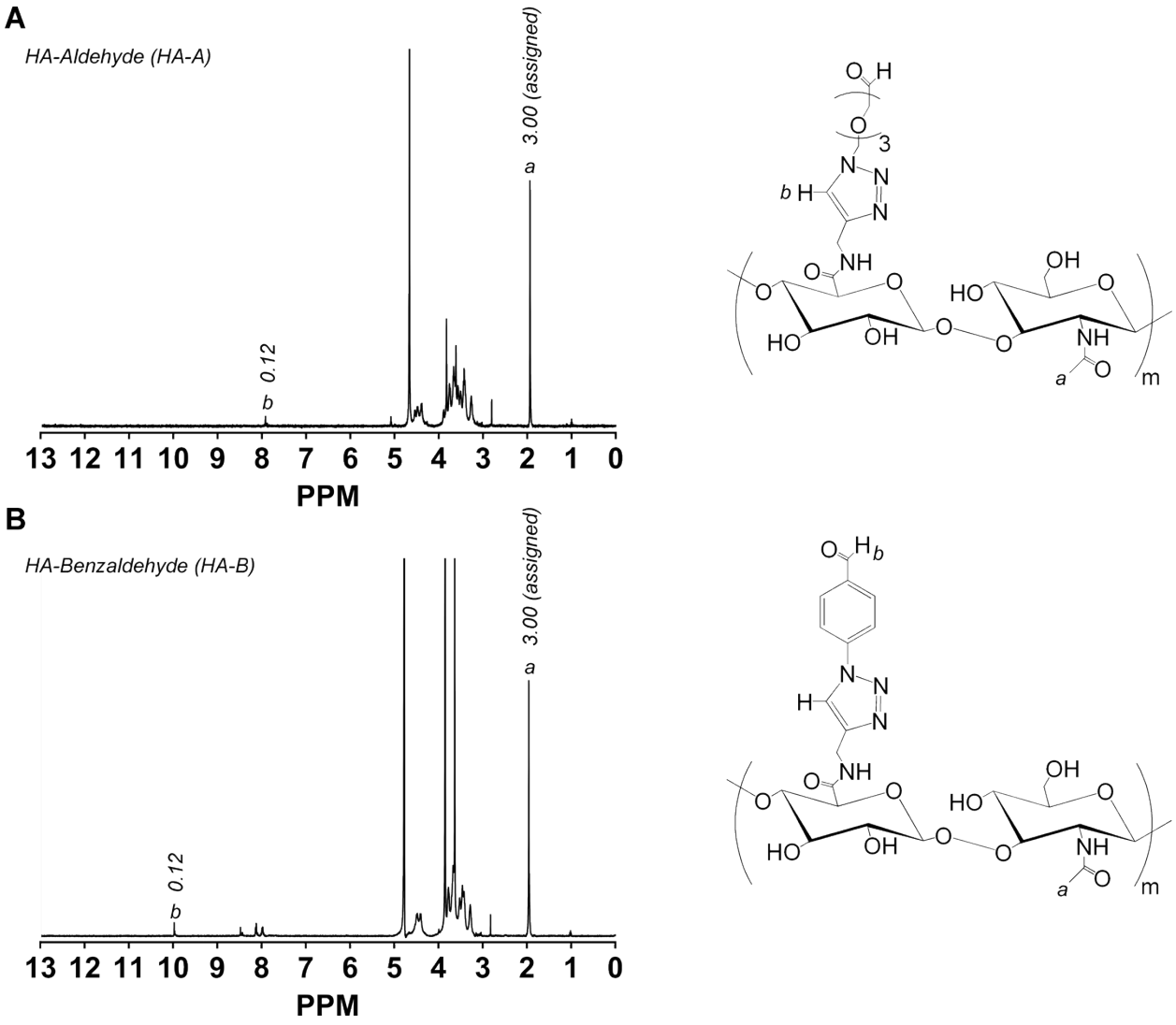

Figure S5: NMR quantification of modification efficiency for aldehyde (HA-A) and benzaldehyde (HA-B) modified HA: *NMR of both (A) HA-A and (B) HA-B show approximately 12% of the available carboxylic acid sites have been modified with eiteher aldehyde or benzaldehyde groups, respectively.*

Gel Permeation Chromatography:

Gel permeation chromatography (GPC) was carried out using a Dionex Ultimate 3000 instrument (including pump, autosampler, and column compartment). Detection consisted of an Optilab TrEX (Wyatt Technology Corporation) refractive index detector operating at 658 nm and a HELEOS II light scattering detector (Wyatt Technology Corporation) operating at 659 nm. The column used was a Superose 6 increase 10/300 GL. The eluent was PBS buffer with 30% (w/v) NaN_3, 137 mM NaCl, 0.0027 mM KCl, 10 mM Phosphate pH 7.3, at 0.75 mL min^{-1} at RT. HA samples of 1.5 MDa, 1 MDa at 1 mg mL^{-1}, and other analyte samples at 3 mg mL^{-1} were dissolved in ultra-pure DI water overnight and filtered through Millipore Express PES membrane filter with 0.22 pore size prior to injection. A refractive index increment (dn/dc) value of 0.165 was applied for all samples. The time frame for integration was determined by running multiple unmodified HA samples (20 kDa, 40 kDa, 60 kDa, 100 kDa, 500 kDa, 1 MDa; (Lifecore), and 1.5 MDa (Sigma)) as a reference and then applying the same integration time for our experimental samples (HA24, HA16, HA8, HA-A, and HA-B). Values represent the approximated weight average molecular weight (M_w), number average molecular weight (M_n) and the polydispersity index (PDI).

Dynamic Light Scattering for Measuring Hydrodynamic Radius:

50 µL of each HA sample were dissolved in PBS at a final concentration of 1% (w/v). Then, 40 µL of sample were transferred into disposable cuvettes (BrandTech, 759200) and sealed with a cap (VWR, 47744-636) to prevent any evaporation during measurements. We then performed a size measurement using the Zetasizer Nano NS, with three replicate measurements per sample. From these measurements, and assuming the viscosity of water, we were able to determine the z-average size for each sample from which we could then determine an approximate hydrodynamic radius (R_h). The R_h values provided presently represent the average of three independent, samples.

A

Gel Permeation Chromatography			
HA-Variant	**Mw, obs.**	**Mn, obs.**	**PDI**
1.5 MDa	*1.24 MDa*	*1.23 MDa*	*1.01*
1 MDa	*1.11 MDa*	*1.05 MDa*	*1.05*
500 kDa	*345.0 kDa*	*324.0 kDa*	*1.07*
100 kDa	*101.0 kDa*	*95.2 kDa*	*1.15*
60 kDa	*60.4 kDa*	*42.2 kDa*	*1.43*
40 kDa	*59.7 kDa*	*44.0 kDa*	*1.36*
20 kDa	*19.8 kDa*	*14.2 kDa*	*1.40*
*HA-B**	*141.0 kDa*	*119.0 kDa*	*1.19*
*HA-A**	*221.0 kDa*	*161.0 kDa*	*1.37*
HA8	*177.0 kDa*	*143.0 kDa*	*1.24*
HA16	*80.1 kDa*	*57.3 kDa*	*1.41*
HA24	*56.8 kDa*	*43.9 kDa*	*1.30*
HA-Alkyne	*113.0 kDa*	*86.0 kDa*	*1.30*

B

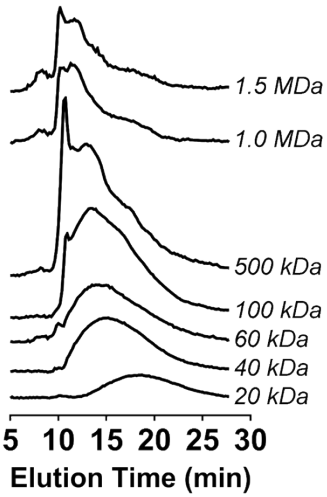

C

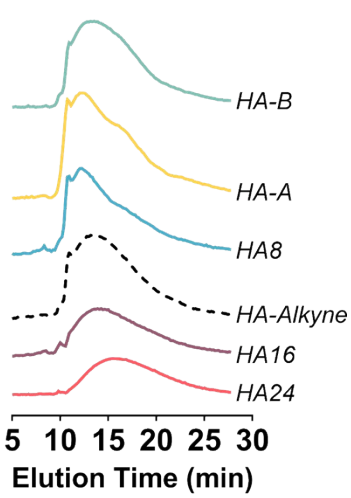

D

Dynamic Light Scattering	
HA-Variant	**Hydrodynamic Radius**
1.5 MDa	*45.39 nm ± 2.645 nm*
1 MDa	*26.69 nm ± 0.497 nm*
500 kDa	*15.83 nm ± 0.632 nm*
100 kDa	*10.56 nm ± 0.123 nm*
60 kDa	*9.73 nm ± 0.518 nm*
40 kDa	*9.61 nm ± 0.183 nm*
20 kDa	*8.10 nm ± 0.705 nm*
*HA-B**	*11.51 nm ± 0.871 nm*
*HA-A**	*14.48 nm ± 0.234 nm*
HA8	*12.91 nm ± 1.36 nm*
HA16	*7.45 nm ± 0.379 nm*
HA24	*7.09 nm ± 0.109 nm*
HA-Alkyne	*10.95 nm ± 0.526 nm*

E

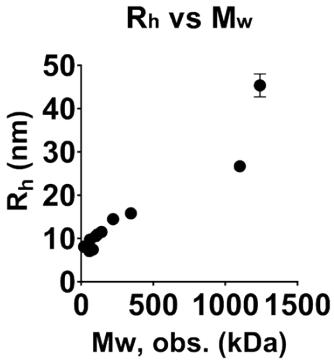

F

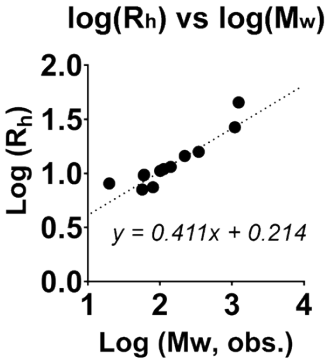

Figure S6. Gel permeation chromatography (GPC) measurements of hyaluronans: *To characterize the molecular weight (M_w) of our different hyaluronan (HA) variants, we used gel-permeation chromatography (GPC) on both reference unmodified H, and our experimental HA groups. (A) Tabulated results showing the observed weight-average molecular weight (M_w, obs.), number-average molecular weight (M_n, obs.), and polydispersity index (PDI) are shown. GPC measurements were able to accurately determine the molecular weight of our unmodified control groups. HA modified by copper click chemistry (HA-B* and HA-A*) appeared to increase in molecular weight, but this is likely due to the presence of bulky side groups increasing their hydrodynamic radii and inflating the measured value. As expected, oxidized HA samples (HA8, HA16, and HA24) decreased greatly from their starting molecular weight (1.5 MDa) as*

a function of oxidation time. Representative GPC curves have been provided for (B) unmodified HA and our (C) experimental HA groups. Note: *we used a specific refractive index increment (dn/dc) value of 0.165 to calculate the approximate values for all samples. (D) Using dynamic light scattering (DLS) we measured the hydrodynamic radii of unmodified HA controls and our modified HA groups. The hydrodynamic radius (R_h) and the M_w, obs. have been plotted both as (E) linear plots and (F) log-log plots*.

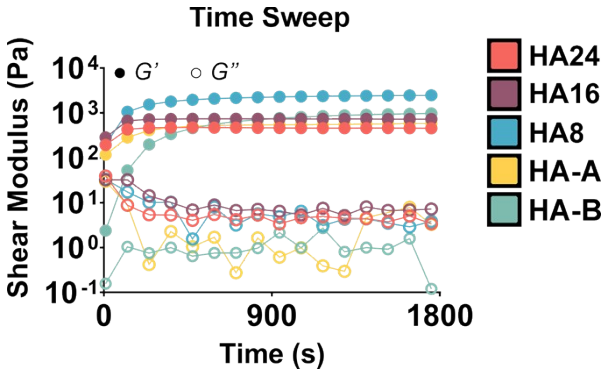

Figure S7. Representative time sweeps: *Following mixing, our five gel formulations (all: 2% (w/v) ELP, 1% (w/v) HA) were crosslinked for 30 min at room temperature. All five formulations began to gel almost immediately following mixing, and all formulations (except HA-B) had a storage modulus (G') > loss modulus (G") prior to the start of measurement. Typical plateau moduli following crosslinking were as follows: ~450 Pa for HA24; ~730 Pa for HA16; ~2500 Pa for HA8; ~590 Pa for HA-A; ~ 980 Pa for HA-B.*

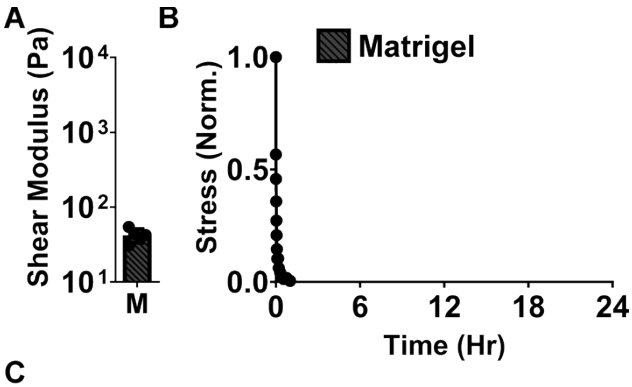

C

Matrigel Mechanics		
Hydrogel	**Shear Modulus**	**$t_{0.5}$**
Matrigel	*~ 39 Pa*	*~ 67.0 s*

Figure S8. Summary of Matrigel mechanics: *Summary mechanics of Matrigel using our prescribed mechanical testing protocols. We found that Matrigel has a shear modulus of ~39 Pa and a stress relaxation, as denoted by $t_{0.5}$, of ~67.0 s.*

Measuring Lower Critical Solution Temperature:

The lower-critical solution temperatures (LCST) of our proteins were measured by taking absorbance measurements (λ = 300 nm) in a circular dichroism (CD) spectrometer (J-1000, JASCO). Briefly, a 250 μL sample of 1% (w/v; 10 mg mL-1) ELP both pre- and post-functionalization was made by dissolving lyophilized protein in 1X PBS overnight at 4 °C on a constant rotator. The following morning, 200 μL of freshly dissolved sample was loaded into a pre-chilled (4 °C) 1-mm band-width quartz cuvette and then loaded into the CD spectrometer sample chamber. The absorbance spectra were measured at 1 °C increments over the temperature range 4 °C - 65 °C. To ensure adequate incubation, the temperature was elevated at 1 °C min^{-1} and held at each degree increment for 30 seconds. To approximate the LCST for each sample, we first subtracted away a blank (PBS only) scan collected using the same protocol. Then, we normalized the curves by dividing each absorbance measurement collected by the maximum absorbance value over the length of the measurement. The LCST temperature range is defined as the approximate temperature where absorbance (norm.) = 0.5.

A

LCST Shift with Functionalization		
Protein	**Moiety**	**LCST (°C)**
ELP	*Unmodified*	*33 - 34*
ELP-Hyd	*Hydrazine*	*38 - 39*

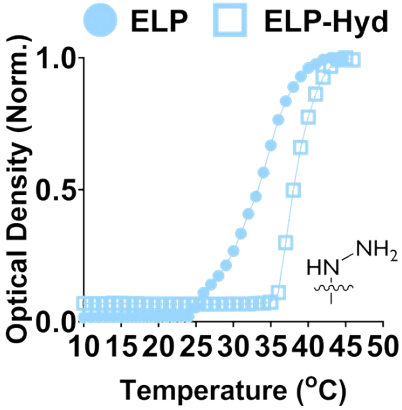

B

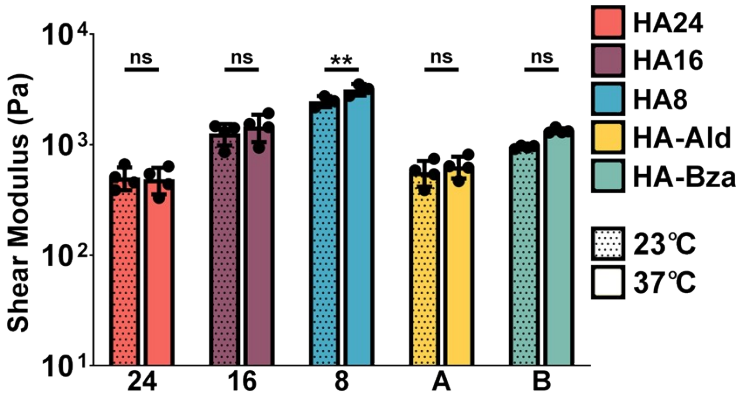

Equilibrium Shear Modulus					
HA-Variant	*HA24*	*HA16*	*HA8*	*HA-Ald*	*HA-Bza*
23 °C	*~500 Pa*	*~1300 Pa*	*~2500 Pa*	*~560 Pa*	*~1000 Pa*
37 °C	*~490 Pa*	*~1500 Pa*	*~3200 Pa*	*~640 Pa*	*~1300 Pa*

Figure S9. Lower critical solution temperature (LCST) shift: *(A) The lower critical solution temperature measurements of ELP pre- and post-modification with hydrazine moieties. (B) Shear moduli of crosslinked gels at ambient (23 ˚C) and body (37 ˚C) temperatures. 2-Way ANOVA multiple comparison's test, α = 0.05, post-hoc Bonferroni test, ** p < 0.01, ns = not significant.*

Note: These videos have been uploaded as separate files. A brief description is listed below.

Figure S10. Representative injection videos: *(A) Representative video of injecting 50 µL of HA24 (dyed red with food coloring for ease of visibility), (B) HA16 (dyed purple with food coloring for ease of visibility), (C) HA8 (dyed blue with food coloring for ease of visibility), (D) HA-A (dyed yellow with food coloring for ease of visibility), and (E) HA-B (dyed green with food coloring for ease of visibility) through a 30-G, manually hooked, needle by hand*

Note: This video has been uploaded as a separate file. A brief description is listed below.

Figure S11. Catheter injection video of HA16: *To screen the potential for translatability of our hyaluronan and elastin-like protein (HELP) gel system, we tested the injection of 700 µL HA16 (dyed dark green for ease of visibility) through a 150-cm catheter. Injections were done by hand.* Note: *the beginning of the video has been accelerated (x8). Total injection time is 3 min and 8 sec. For reference, the 30-G needles used in our study had an injection length of 0.8 cm and an 0.159 mm inner diameter compared to the Codman catheter which was 150 cm in length and had an inner diameter of 0.75 mm.*

Post-Injection Mechanics Test:

50 µL of hydrogel were prepared as previously described and loaded into the back of a 30-G syringe. Hydrogels were crosslinked for 30 min and then injected, by hand, onto an ARG2 rheometer (TA Instruments). Post-injection recovery was monitored at 1% strain and radial frequency of 1 rad s^{-1} over the course of 24 hr. Heavy mineral oil was used to fill the gap between the rheometer geometry and external environment to ensure hydration over the course of all measurements. Immediately following the 24-hr recovery period, the shear modulus for each sample was measured at 23 °C using a non-destructive frequency sweep over the oscillatory frequency range of 0.1 - 10 rad s^{-1} at a fixed strain of 10%.

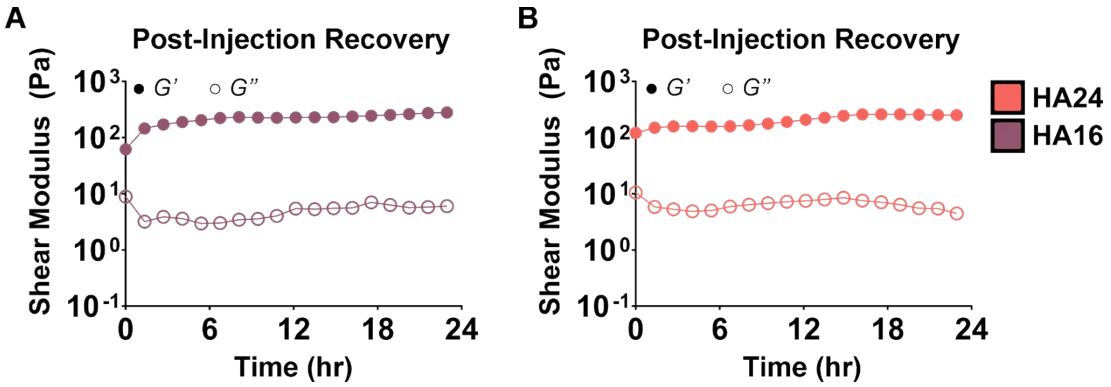

Figure S12. Recovery experiment for HA16 and HA24: *24-hr recovery experiment of 50 µL of (A) HA16 and (B) HA24 post-injection at 1% strain and a frequency of 1 rad s^{-1}.*

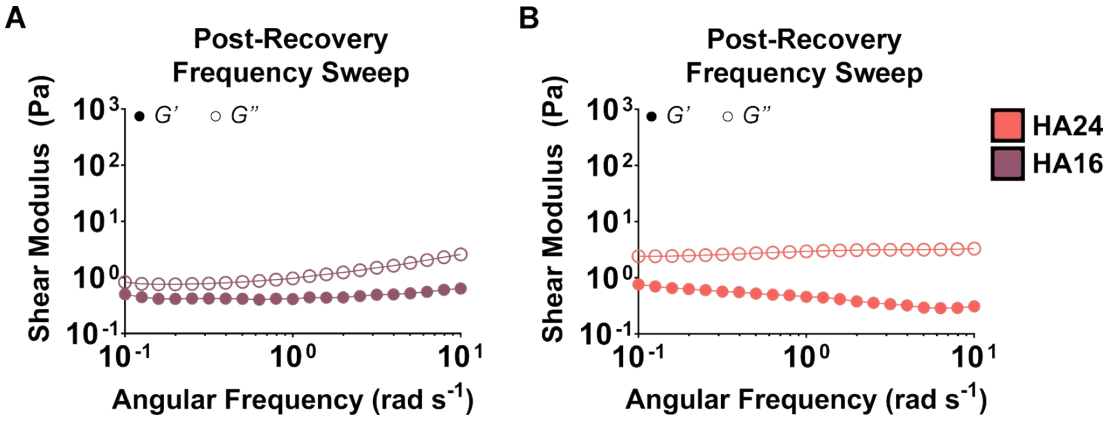

Figure S13. Post-recovery frequency sweep: *After 24-hr of recovery post-injection we measured shear stiffness of (A) HA16 and (B) HA24 via a frequency sweep at 10% strain and over a range of 0.1 rad s^{-1} to 10 rad s^{-1}, as detailed in the methods section.*

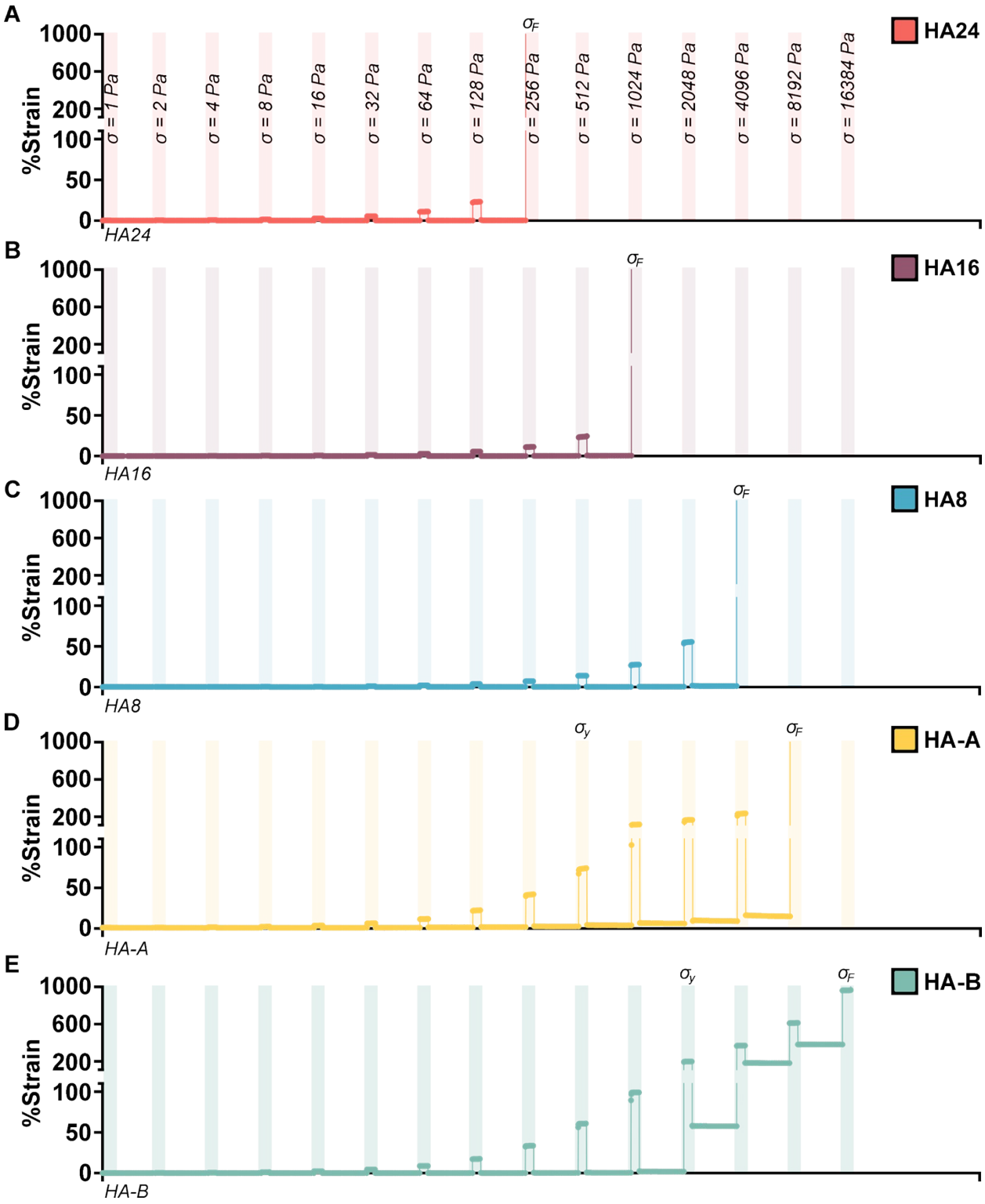

143 **Figure S14. Representative stress and strain curves:** *Representative failure stress measurement tests*
144 *for (A) HA24, (B) HA16, (C) HA8, (D) HA-A, and (E) HA-B showing the measured strain over successive*
145 *stress steps (demarcated by a semi-transparent bar and corresponding stress) and relaxation steps. The*

x-axis, for all plots indicates time (s), plotted linearly. The stress required to induce fracture is indicated by σ_F*. Note that the y-axis is broken into two parts: (1) 0 – 100 % strain and (2) 100 – 200% strain. The oxidized HELP (HA24, HA16, and HA8) groups reached much lower strain values (< 50%) prior to failure than the bio-conjugated variants, HA-A and HA-B, which experienced % strain > 100% prior to failure. Additionally, both HA-A and HA-B had evidence of a yielding behavior (% strain >> 0 post-relaxation (*$\sigma = 0$*)) and are denoted with a* σ_y*.*

Labeling ELP with Cyanine 5

To aid with the visualization of our HELP hydrogels post-injection, we labeled a single lysine group on a portion of our ELPs with a cyanine 5 (Cy5) NHS molecule (excitation: 651, emission: 670; Sigma 679011) via standard NHS-ester chemistry. Briefly, ELP was dissolved in anhydrous DMSO at an initial concentration of 6% (w/v) at room temperature (RT) under constant rotation. After dissolving, the reaction volume was diluted further with anhydrous DMF, dropwise, to a final concentration of 2% (w/v). Next, a 1 molar equivalent of activated Cy5-NHS ester was dissolved in anhydrous DMF (100 mg mL^{-1}) and added dropwise to the 2% (w/v) ELP reaction mixture. Once added, the reaction vile was purged with nitrogen gas for 5 ~ 10 min. After purging, the reaction vile was covered with aluminum foil to prevent photo bleaching and the reaction was allowed to proceed overnight at RT.

To isolate the modified ELP-Cy5, the reaction volume was added, dropwise, into ice-cold diethyl ether to a final volumetric ratio 1:5 (reaction: ether) in a solvent-safe centrifugation tube. ELP-Cy5 was then collected by centrifugation (>18000 x *g*) at 4 °C for 30 min, decanted, and dried overnight. The dried ELP-Cy5 product is then dissolved in ultra-pure DI water at a final concentration of 2% (w/v) and dialyzed against 4 L of ultra-pure DI. The 4 L of dialysis water was routinely refreshed every 12 hr over the course of 3 days. The final dialyzed product was then sterilized using a 0.22-μm syringe filter, frozen, and finally lyophilized for 3 days in a sterile, filtered 50-mL tube. To verify the degree of functionalization, ELP-Cy5 can be characterized via NMR (below). If the ELP molecule has been sufficiently modified (~ 1 Cy5 molecule per ELP), ELP-Cy5 can be further modified with a hydrazine molecule (ELP-Cy5-Hyd) following the previously listed protocol and incorporated into standard HELP gels to reach a desired level of fluorescence.

NMR Quantification:

Cy5 Functionalization: dissolve ~10 mg of ELP-Cy5 in ~750 μL of deuterated DMSO and analyze by 1H NMR (500 Hz, DMSO-d6): Tetramethyl silane (TMS; 0). Efficiency of modification is

177 determined by comparing the integrated signal of the lysine peak (δ 2.75-1.65; unmodified 28H)
178 to the aromatic protons of tyrosine residues on ELP (8H each; centered around δ 7.00 and 6.62,).

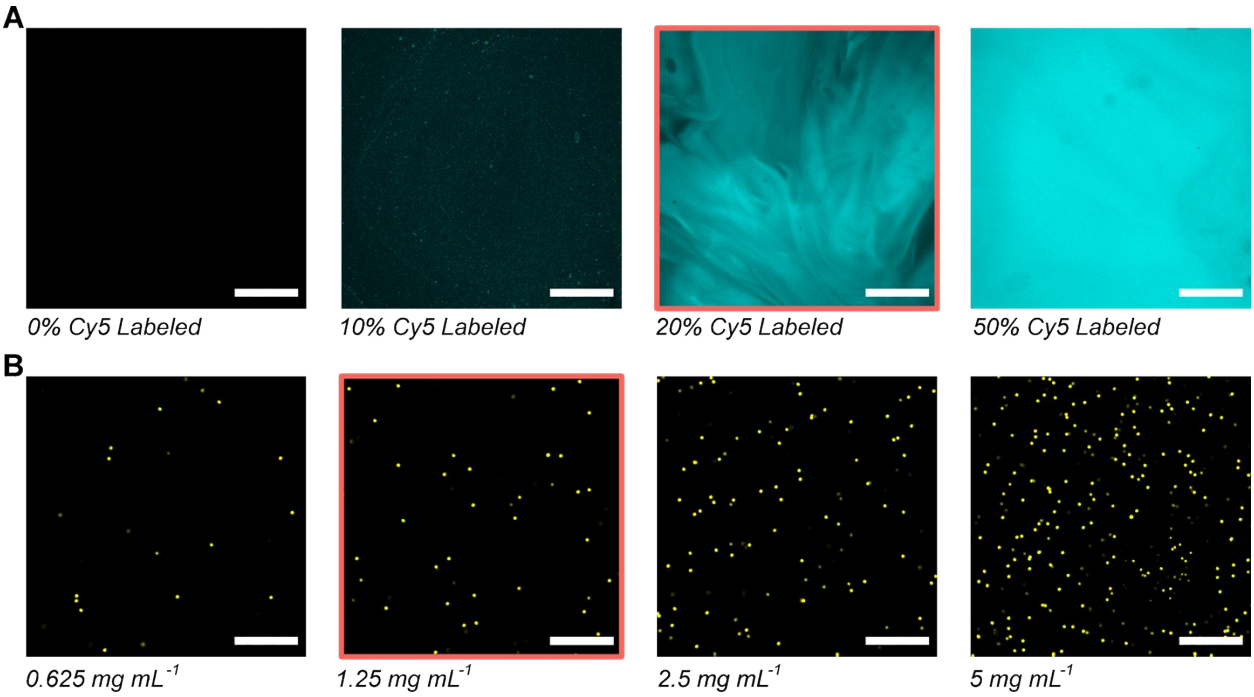

Figure S15. *Ex vivo* hydrogel fluorescence and microsphere concentration determination: *To identify an appropriate level of ELP-cyanine-5 labeling and microsphere concentration for subsequent* in vivo *experiments, we prepared HELP gels with varying levels of (A) volume percent labeled ELP and (B) concentration of fluorescent microparticles. From our* ex vivo *screening, we opted to use 20% (v/v) ELP-Cy5-Hydrazine and 1.25 mg mL^{-1} 10-μm fluorescent particles (selections are outlined in red). Based on this image, we further estimated that a 50-μL injection would have approximately ~70,110 microspheres.* Note: *all images represent 20-μm thick z-stacks to emulate the intended tissue thickness; all scale bars denote 250 μm.*

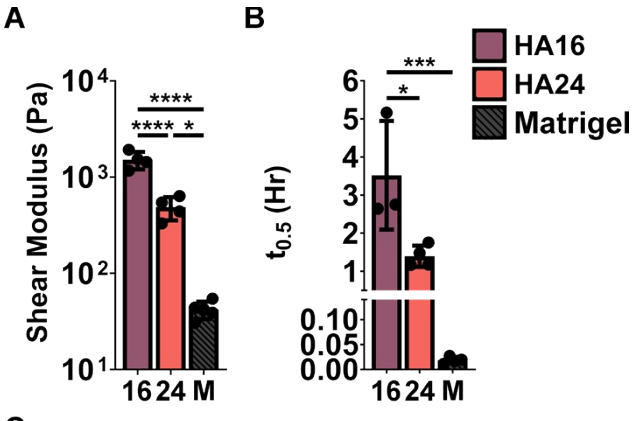

C

Test Group Gel Mechanics		
Hydrogel	**Shear Modulus**	**$t_{0.5}$**
HA16	*~ 1500 Pa*	*~ 3.5 hr*
HA24	*~ 490 Pa*	*~ 1.4 hr*
Matrigel	*~ 39 Pa*	*~ 67.0 s*

All data previously shown

Figure S16. Summary of test group mechanics: *Summary of the (A) shear moduli and (B) stress relaxation rates of HA16, HA24, and Matrigel. (C) Average values are reported for ease of comparison. Note: these data have been previously shown, but are recompiled here for ease of direct comparison. Collectively, these gels established "low" (~40 Pa), "medium" (~500 Pa), and "high" (~1500 Pa) stiffness gels for our* in vivo *retention study. Statistical test: one-way ANOVA, α = 0.05, post-hoc Tukey test. * p < 0.05; *** p < 0.001; **** p < 0.0001.*

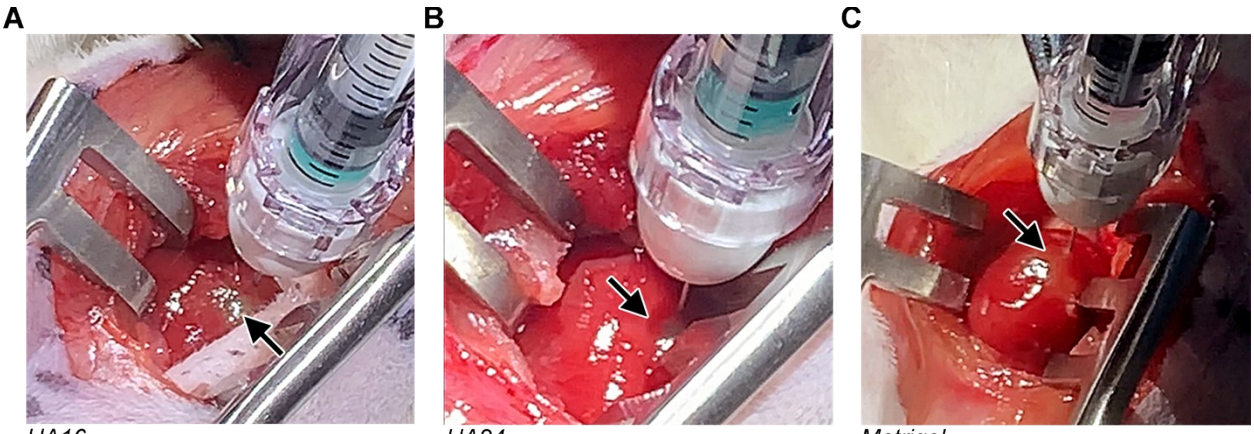

Figure S17. Representative injection images: *Representative images showing injections of 50 µL of (A) fluorescently labeled HA16, (B) fluorescently labeled HA24, and (C) Matrigel, each with a final concentration of 1.25 mg mL^{-1} 10-µm fluorescent microspheres. Arrows indicate evidence of material injection of the material, indicated by the formation of a bolus and slight discoloration of the tissue.*

Injection Scoring Procedure:

For injection scoring, we devised a 4-part scoring system that assessed clinically relevant concerns in cardiothoracic surgical injection paradigms: (1) the observable amount of material reflux (on a scale of 0 - 3 points ranging from no visibly remaining material to no material reflux), (2) ease of injection (on a scale of 0 - 3 points ranging from no smoothness in injection to controlled smooth injection), (3) degree of bleeding post-injection (on a scale of 0 - 3 points ranging from excessive bleeding with risk of death to no spot bleeding), and (4) correct location of the injection site (on a binary scale of 0 - 1 point with the injection visually being in the incorrect or correct location). These scores were tabulated for each gel group at both time points for a total possible score of 10 points. Scores were assigned by an external observer, blind to the injection group and time point.

A

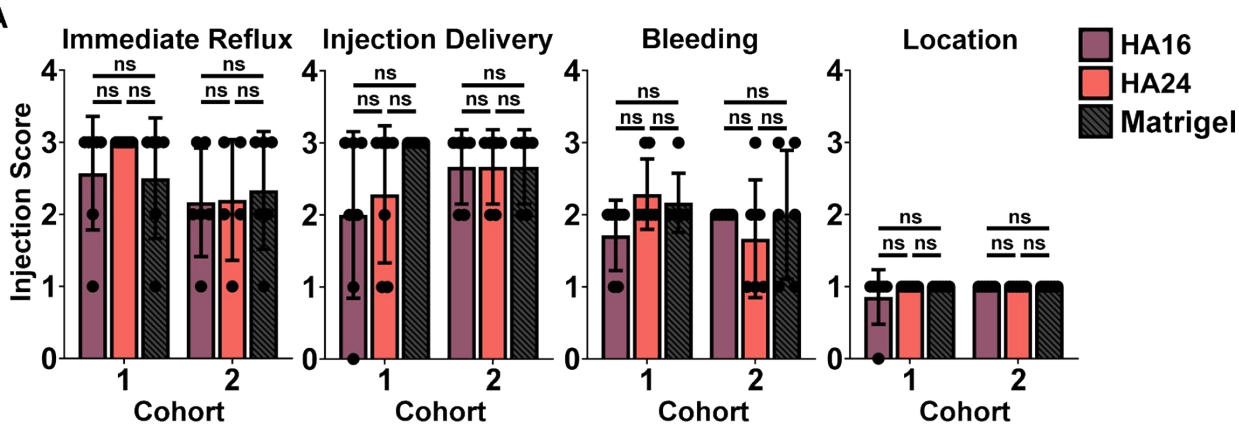

B

In Vivo Injection Scoring : Immediate Reflux	
Score	*Description*
0	*No sign of material retained at injection site.*
1	*Severe material reflux.*
2	*Mild material Reflux.*
3	*No visible material reflux.*

C

In Vivo Injection Scoring : Injection Delivery	
Score	*Description*
0	*Challenging injection, uneven or "jerky".*
1	*Severe "jerkiness" in injection.*
2	*Mild "jerkiness" in injection.*
3	*Smooth, even injection.*

D

In Vivo Injection Scoring : Bleeding	
Score	*Description*
0	*Severe bleeding, pooling in chest cavity.*
1	*Mild bleeding, long clot time.*
2	*Light spot bleeding.*
3	*No spot bleeding.*

E

In Vivo Injection Scoring : Location	
Score	*Description*
0	*Incorrect location or depth (shallow).*
1	*Correct location and depth.*

Figure S18. Injection scoring: *To probe the possibility that retention could be influenced by the quality of our injections, we devised a 4-part scoring system that looked at: (1) the observable amount of reflux, (2) ease of injection, (3) degree of bleeding post-injection, and (4) correct location of the injection site. (A) These scores were tabulated for each gel group for both cohorts, 1 and 7 day time points post-injection, respectively. Scores were assigned by an external observer, blind to the injection group and time point. (B – D) A breakdown of the scoring scheme has been provided for reference. Notably, we found no significant differences in the quality of our injections between our groups. Statistical test: two-way ANOVA, α = 0.05, post-hoc Tukey test, not significant = n.s.*

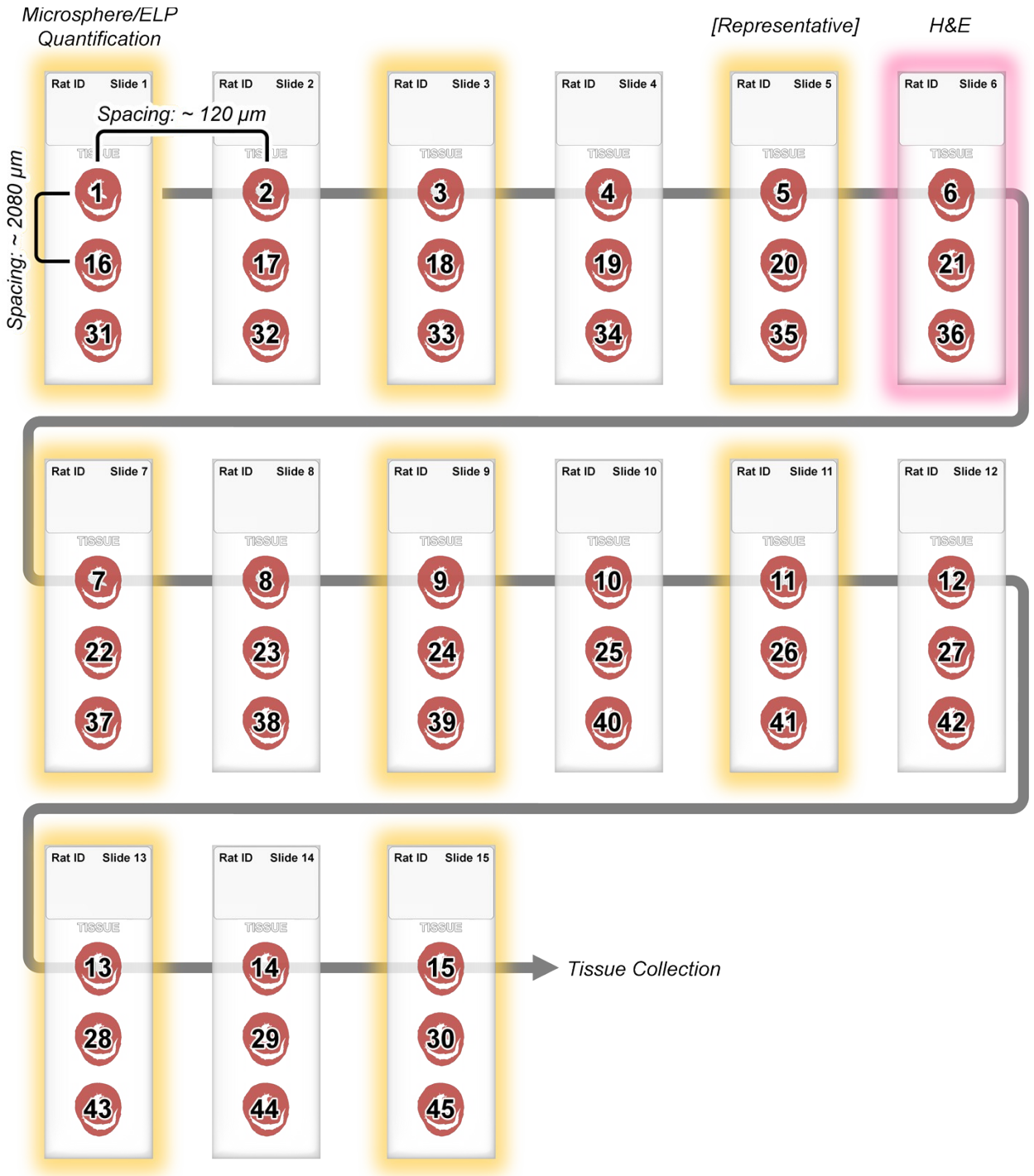

218 **Figure S19. Tissue sectioning schematic:** *To maintain a consistent and unbiased survey of our different*
219 *test groups, all tissues were sectioned and sampled according to the above scheme. Briefly, 15 gelatin-*
220 *coated slides were collected from each animal for analysis. Serial slices (20-μm thick) of heart tissue were*
221 *made, and every seventh slice was collected; i.e., slides were prepared from tissue slices spaced*

approximately ~120-μm apart. Importantly, the exact number of tissue slices between each collected tissue sample was recorded and used in the final quantification. In the above diagram, we have numbered each tissue section (1 – 45) to reflect the general ordering of sample collection, where the first 15 samples (1-15) were placed at the top of each slide, the next 15 samples (16 – 30) were collected in the middle row, and the last 15 were collected on the bottom row (31 – 45). By sectioning tissue this way, each slide spanned approximately 4 mm in height and provided a rapid way of surveying a large amount of tissue with relatively few slides needing to be imaged. From the 15 total slides, 8 (slides 1, 3, 5, 7, 9, 11, 13, and 15) were collected from each animal and imaged for microspheres and elastin-like protein (ELP) according to our described methods. To select a slide for Hematoxylin & Eosin (H&E) staining, we designated from those 8 slides one that was 'representative' (having qualities numerically and morphologically indicative of that particular injection) and a slide adjacent to that was then selected for histological staining.

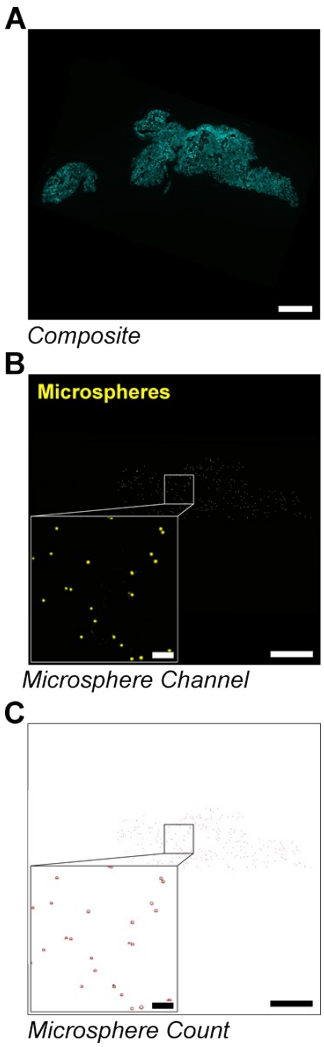

Figure S20. Example images of microsphere retention quantification: *Tabulation of microsphere count was carried out by automated quantification of fluorescent images. (A) First, 45, 20-μm thick, tissue sections were extracted semi-periodically with a cryostat from a larger 5-mm section of rat heart collected and fixed according to our previously stated methods (see* ***Figure S19****). Tissue sections were imaged with aid of an inverted fluorescent microscope for evidence of injected cargo: ELP and/or fluorescent microspheres. (B) From composite images we isolated the microsphere channel and saved them from each tissue slice. (C) These images were then converted to binary images (using a constant threshold value) and the number of microspheres were tallied for each slice using a particle counter in ImageJ. To generate more accurate counts, tallies from each image slice were then checked for instances of 'clustering' (multiple microspheres being counted as one) by a secondary Python script that divided the cross-sectional area of each microsphere by the average area of an individual microsphere, and extra counts were added*

accordingly for each slice. Note: scale bar on low magnification images represents 1 mm, scale bar on high-magnification images represents 100 μm.

Note: This file has been uploaded separately. A brief description is listed below:

Figure S21. Python script for post-processing microsphere count: *A Python script was written and used to account for microsphere 'clustering' which superficially undercounted the number of microspheres in our captured images.*

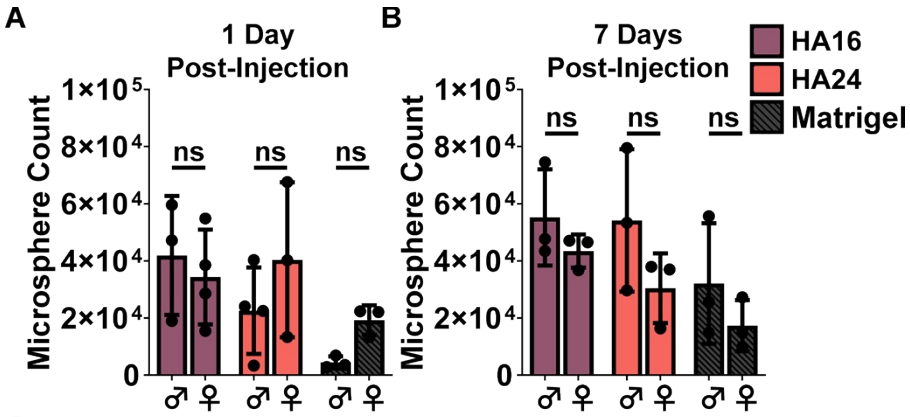

C

Average Microsphere Count, by Sex								
	1 Day Post-Injection				7 Days Post-Injection			
Hydrogel	♂	n	♀	n	♂	n	♀	n
HA16	*~42000*	*3*	*~34000*	*4*	*~55000*	*3*	*~43000*	*3*
HA24	*~23000*	*4*	*~40393*	*3*	*~54000*	*3*	*~30000*	*3*
Matrigel	*~4400*	*3*	*~19000*	*3*	*~32000*	*3*	*~17000*	*3*

Figure S22. Sex-based differences in microsphere retention: *To investigate the possibility of any sex-related differences, we plotted the average microsphere count for each hydrogel, by sex, for both (A) 1 day and (B) 7 days post-injection. Importantly, we did not observe any significant differences based on sex. Generally, it appeared that male rats had a greater degree of retention, but not in a statistically significant manner. (C) The results have been additionally summarized for reference. Statistical test: two-way ANOVA, α = 0.05, post-hoc Tukey test, not significant = n.s.*

Supplemental References:

[1] Y.-C. Chen, W.-Y. Su, S.-H. Yang, A. Gefen, F.-H. Lin, In situ forming hydrogels composed of oxidized high molecular weight hyaluronic acid and gelatin for nucleus pulposus regeneration, Acta Biomater. 9 (2013) 5181–5193. https://doi.org/10.1016/j.actbio.2012.09.039.